http://dx.doi.org/10.5935/0103-5053.20130295

J. Braz. Chem. Soc., Vol. 25, No. 2, 282-289, 2014.
Printed in Brazil - ©2014 Sociedade Brasileira de Química
0103 - 5053 $6.00+0.00

Article

Variable-Temperature NMR and Conformational Analysis of Oenothein B

Suzana C. Santos, Ariadne G. Carvalho, Gilmara A. C. Fortes, Pedro H. Ferri and Anselmo E. de Oliveira*

Instituto de Química, Universidade Federal de Goiás, C.P. 131, 74001-970 Goiânia-GO, Brazil

Oenoteína B é um tanino hidrolisável dimérico com um amplo espectro de atividades biológicas, tais como antitumoral, anti-inflamatória e anti-viral. Seus espectros de ressonância magnética nuclear (RMN) à temperatura ambiente apresentam duplicações e alargamento de sinais. Experimentos de RMN uni e bidimensionais a baixas temperaturas foram úteis no assinalamento de todos os sinais de hidrogênios e carbonos sem a necessidade de derivatização. A estrutura tridimensional do confôrmero mais estável foi determinada pela primeira vez através do experimento de espectroscopia de efeito nuclear Overhauser (NOESY) (–20 ºC) e cálculos computacionais usando métodos de teoria do funcional de densidade (DFT) (B3LYP/6-31G) e modelo contínuo polarizado (PCM). A conformação mais favorecida apresentou uma geometria altamente compactada e sem simetria, onde os dois grupos valoneoila mostraram diferentes parâmetros conformacionais e estabilidades.

Oenothein B is a dimeric hydrolysable tannin with a wide range of biological activities, such as antitumour, anti-inflammatory and antiviral. Its nuclear magnetic resonance (NMR) at room temperature show duplications and broadening of signals. Experiments of 1D and 2D NMR at lower temperatures were useful for the complete NMR assignments of all hydrogens and carbons. The 3D structure of the most stable conformer was determined for the first time by nuclear Overhauser effect spectroscopy (NOESY) experiment (–20 ºC) and density functional theory (DFT)(B3LYP/6-31G)/polarizable continuum model (PCM) quantum chemical calculations. The favoured conformation showed a highly compacted geometry and a lack of symmetry, in which the two valoneoyl groups showed distinct conformational parameters and stabilities.

Keywords: oenothein B, variable-temperature NMR, macrocyclic dimer, conformational analysis

Introduction

Oenothein B is a dimeric hydrolysable tannin with a macrocyclic structure (Figure 1) and it is formed by the coupling of two tellimagrandin I units. It was first isolated from the leaves of *Oenothera erythrosepala* and later from several other species,[1] such as *Woodfordia fruticosa*,[2] *Eucalyptus alba*,[3] *E. consideniana* and *E. viminalis*,[4] *Eugenia uniflora*, *Cuphea hyssopifolia* and *Epilobium*.[5]

A wide range of biological activities was described for this compound, including *in vitro* and *in vivo* inhibitory growth of several human carcinoma and leukemia cell lines.[6,7] The oenothein B antitumour activity *in vivo* may be due to the enhancement of the host immune system via induction of IL-1β and the modulation of phagocyte functions.[7,8] Other activities such as inhibition of

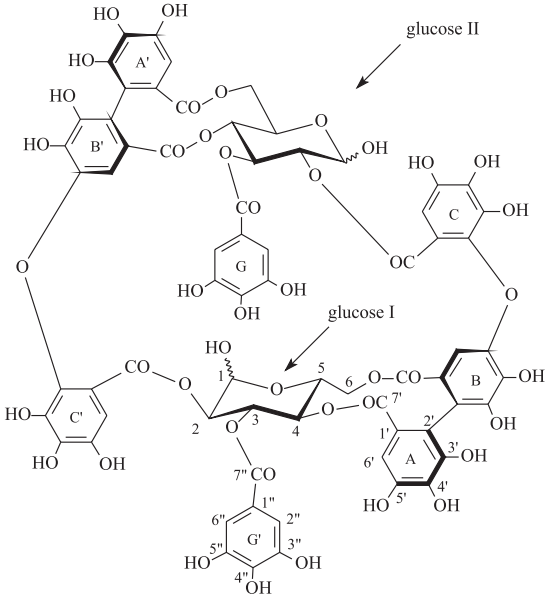

Figure 1. Chemical structure of oenothein B.

*e-mail: suzana.quimica.ufg@hotmail.com

poly(ADP-ribose) glycohydrolase, EBV DNA polymerase and hyaluronidase contribute for the prevention of mouse mammary tumour, nasopharyngeal carcinoma, and confirmed an anti-inflammatory activity, respectively.[9,10] This compound showed potent anti-herpes simplex virus activity and induced morphological changes in the fungus *Paracoccidioides brasiliensis*.[11]

The ^{1}H and $^{13}C\{^{1}H\}$ nuclear magnetic resonance (NMR) spectra spectra at room temperature (20 °C) of macrocyclic ellagitannins, such as oenothein B, woodfordin C, and cameliin B,[1,12,13] are not informative as they show the duplication of each signal due to an anomer-mixture formation and a marked broadening of several aromatic and glucose signals.[13] This phenomenon is caused by the restricted rotation around the ether linkages of the valoneoyl groups, as a consequence of which there is a slow interconversion among meta-stable macro-ring conformations.[1,2,13] The ^{1}H NMR spectra recorded at higher temperatures (38 °C and 50 °C) have been adopted,[13] although it is still not possible to identify clearly all aromatic hydrogens. Methylation of all hydroxy groups with dimethyl sulfate has been another option, as the ^{1}H and $^{13}C\{^{1}H\}$ NMR spectra of some methyl derivatives measured at room temperature exhibited sharp signals.[12,13]

Due to the difficulty in obtaining clear NMR spectra, the structure elucidation of oenothein B was first achieved through several degradation reactions such as total and partial hydrolysis with diluted sulfuric acid, methanolysis of the methyl derivative and the identification of the tetrahydro derivative obtained by the treatment of oenothein B with $NaBH_4$.[1] The ^{1}H and $^{13}C\{^{1}H\}$ NMR spectra of the reduced product were well defined as there is no anomerization equilibrium in the glucitol cores[1,13] and probably the macrocyclic ring becomes less rigid with the opening of the two glucose rings.

The aim of this study was to review ^{1}H and ^{13}C NMR chemical shifts assignments of oenothein B by means of variable-temperature NMR spectroscopy of the non derivatizated compound. In addition, density functional theory/polarizable continuum model (DFT/PCM) theoretical calculations and nuclear Overhauser effect spectroscopy (NOESY) technique were used to investigate the most stable conformation of oenothein B.

Experimental

General

Acetone-d_6 (99.9%) and deuterium oxide (99.9%) were obtained from Cambridge Isotope Laboratories Inc. (Andover, MA, USA). Column chromatography was run using Diaion HP-20 (Supelco) and Sephadex LH-20 (Sigma-Aldrich). Analytical thin-layer chromatography (TLC) was carried out with Silica gel 60 F_{254} (Merck) plates, using formic acid-ethyl formiate-toluene (1:7:1) as the mobile phase. Visualization of TLC spots was performed by spraying with a 1% ethanolic solution of ferric chloride in HCl (0.1%) and UV light. All other chemicals used were of analytical grade.

Compound isolation

Oenothein B was isolated from *E. uniflora* leaves (deposit number UFG 25477). Dried powdered leaves (1 kg) were extracted with 50% acetone at room temperature. After removing acetone by vacuum, the suspended aqueous extract was partionated with ethyl acetate. The aqueous layer was lyophilized to yield a 122 g fraction, which was dissolved in methanol (MeOH) to separate the soluble (86 g) and insoluble (33 g) methanolic fractions. Six portions of the soluble methanolic fraction were submitted to column chromatography over Diaion HP-20 (200 g) with water and aq. MeOH (20% → 40% → 60% → 80%). The 80% MeOH eluate (13 g) was chromatographed over Sephadex LH-20 (200 g), eluted with the same gradient of water and aq. MeOH to afford oenothein B (0.5 g).

NMR spectra

Oenothein B (20 mg) was diluted in acetone-d_6 (0.5 mL) plus two drops of D_2O. Chemical shifts (δ) were given in ppm using TMS as the internal reference and coupling constants (J) were expressed in Hertz. All NMR experiments were recorded on a Bruker Avance III 500 spectrometer operating at 500.13 MHz for ^{1}H and 125 MHz for ^{13}C using 5 mm (TBI) probe. Typical parameter values for ^{1}H measurement were as follows: 3.15 s acquisition time, 9.90 μs 90° pulse width, 1.0 s relaxation delay, 20.6557 ppm spectral width, 32 K matrix size for FT, 32 number of scans and 65536 number of data points. For two dimensional (2D) correlation techniques (COSY, HSQC, HMBC, and NOESY) the typical parameter set was as follows: all data points ($t_2 \times t_1$) were acquired with 4K × 256, an acquisition time of 0.31 s, a relaxation delay of 1.0 s, spectral widths of 250 ppm (^{13}C domain) and 13.15 ppm (^{1}H domain), with 8 to 30 scans per FID. Long-range coupling constant of 10 Hz was set to HMBC experiment. All NMR data were analysed using TOPSIN 2.1 (Bruker BioSpin, 2008).

DFT calculations

The initial oenothein B structure was built using the ACD/ChemSketch program,[14] and geometry optimization

was achieved by the DFT model using the Gaussian09 Rev.A.02 package with the B3LYP hybrid functional and the 6-31G basis set.[15] The solvent effect was simulated by the PCM method, using the integral equation formalism variant (IEF-PCM).[16] The following PCM parameters were used: OFac = 0.8, Rmin = 0.5 Å, Radii = UFF, and solvent = acetone (ε = 20.493). The 3D structure of the final conformer of oenothein B was generated using the Avogrado program.[17]

Results and Discussion

Variable-temperature NMR spectroscopy

The ^{1}H NMR spectrum (acetone-d_6 + D_2O) of oenothein B at room temperature (20 ºC, Figure 2) showed broad signals in the aromatic region (δ 7.30-6.20) and for most of the glucose hydrogens (δ 6.30-3.50). This feature is typical of macrocyclic ellagitannins, in which interconversion among conformational structures is very slow. Furthermore, the balance of anomeric forms in both glucose cores increases spectrum complexity.

NMR experiments are often recorded at high temperatures to overcome the problem of rotation energy barrier. Given the fact that biflavonoid type molecules gain resolution with this procedure, clean ^{1}H NMR spectra were obtained at 80 ºC and 120 ºC for flavanone-(3→8'')-flavone type biflavonoids.[18] In the case of oenothein B, there is an improvement of ^{1}H NMR spectrum at 38 ºC (Figure 2), the glucose hydrogen signals at δ 4.90 (t, H-4$_{II}$), 4.58 (dd, H-5$_I$), 4.15 (dd, H-5$_{II}$), 3.85 (d, H-6$_{II}$), and 3.66 (d, H-6$_I$) became sharper, as well as the aromatic hydrogens at δ 7.02, 6.66, and 6.31. However, even at 50 ºC,[13] not all aromatic hydrogen signals are clearly distinguished.

A sharper definition for the aromatic signals of oenothein B was achieved when running ^{1}H NMR spectra at temperatures from −10 ºC to −30 ºC (Figure 2). Hydrogen and carbon signals usually broaden at lower temperatures, as can be seen for esters of 4-hydroxy-cyclohexanone.[19] However, for some macrocyclic compounds, their spectra increase in sharpness, as is the case of cyclopeptides, tetranitroazacalix[4]arenes, and (+)-germacrene A.[20] At low temperatures, interconversion among conformers slows down, and the most stable macrocyclic conformer may be favoured. Therefore, oenothein B hydrogen and carbon signals were assigned through COSY, HSQC, and HMBC 2D-NMR experiments at −20 ºC (Tables 1 and S1), as in this temperature most glucose hydrogens and all aromatic signals were well defined.

Comparison of the ^{1}H NMR spectra at 20 ºC and −20 ºC showed that some glucose and aromatic hydrogen signals were temperature-dependent (Figure 2). These changes in hydrogen chemical shifts could be explained by the anisotropic shielding/deshielding effects of aromatic rings and ester carbonyls. These effects probably change during temperature reduction, as a consequence of the conformational interconversions and the progressive adoption of a preferred conformation at −20 ºC.

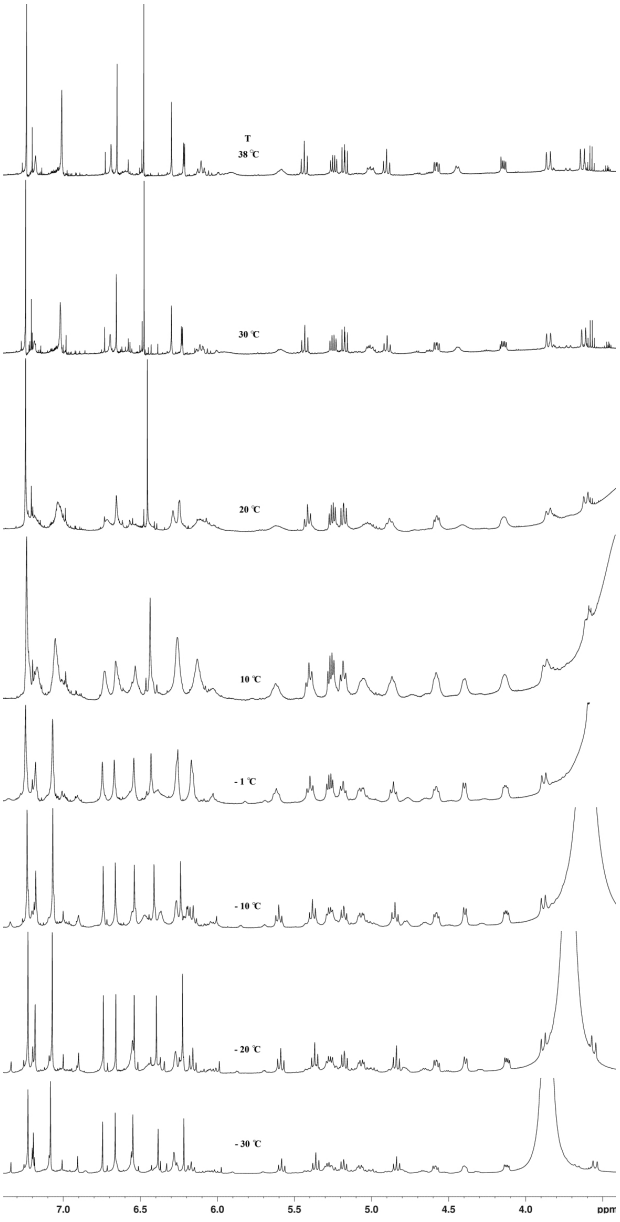

Figure 2. Variable-temperature ^{1}H NMR (acetone-d_6 + D_2O, 500 MHz) spectra for oenothein B.

The changes and sharpness of aromatic hydrogen signals at −20 ºC, especially the separation of hydrogen singlets from A and C' rings, were useful to revise previous hydrogen assignments, which were inverted.[2,4] The two sets of hydrogen signals from each valoneoyl group were assigned based on the detailed analysis of

Table 1. ^{1}H and ^{13}C NMR (500 and 125 MHz, respectively) data for oenothein B (acetone-d_6 + D_2O, −20 °C)

Position	δ_H (m, *J* / Hz)	δ_C	Position	δ_H (m, *J* / Hz)	δ_C
Glucose I[a]			Glucose II[b]		
1	6.28 (br[c])	91.2	1	4.40 (d, *J* 8)	95.5
2	6.18 (d, *J* 10)	74.4	2	5.18 (t, *J* 9)	74.4
3	6.16 (t, *J* 10)	71.2	3	5.38 (t, *J* 10)	73.4
4	5.59 (t, *J* 10)	70.1	4	4.84 (t, *J* 10)	73.9
5	4.58 (dd, *J* 7, 10)	68.6	5	4.13 (dd, *J* 5, 10)	71.6
6	5.27 (dd, *J* 7, 13)	62.8	6	5.07 (dd, *J* 5, 13)	65.2
	3.56 (d, *J* 13)			3.89 (d, *J* 13)	–
Valoneoyl (ring A)			Valoneoyl (ring A')		
1'	–	[d]	1'	–	[d]
2'	–	114.5	2'	–	116.3
3'	–	[d]	3'	–	[d]
4'	–	136.2	4'	–	136.4
5'	–	144.8	5'	–	145.3
6'	6.40 s	107.1	6'	6.67 s	106.8
7'	–	168.1	7'	–	169.4
Valoneoyl (ring B)			Valoneoyl (ring B')		
1'	–	[d]	1'	–	[d]
2'	–	117.2	2'	–	120.9
3'	–	[d]	3'	–	[d]
4'	–	135.2	4'	–	140.1
5'	–	147.2	5'	–	147.0
6'	6.23 s	105.1	6'	7.19 s	113.6
7'	–	167.3	7'	–	167.4
Valoneoyl (ring C)			Valoneoyl (ring C')		
1'	–	[d]	1'	–	[d]
2'	–	143.3	2'	–	142.6
3'	–	[d]	3'	–	[d]
4'	–	134.0	4'	–	138.4
5'	–	139.1	5'	–	138.4
6'	6.75 s	108.6	6'	6.55 s	108.3
7'	–	167.1	7'	–	168.4
Galloyl (ring G)			Galloyl (ring G')		
1"	–	120.7	1"	–	121.4
2"	7.23 s	110.3	2"	7.08 s	110.1
3"	–	145.5	3"	–	145.5
4"	–	138.6	4"	–	138.6
5"	–	145.5	5"	–	145.5
6"	7.23 s	110.3	6"	7.08 s	110.1
7"	–	166.0	7"	–	167.8

[a]α-anomer is predominant; [b]β-anomer is predominant; [c]broadened signal; [d]unidentified carbon signals.

the ^{1}H-^{13}C long-range correlation map from HMBC NMR experiment, in which long-range correlations between aromatic hydrogens and carbons were crucial to discriminate the different rings (Table S1). Hydrogens from A/A' (δ 6.40, 6.67) and B/B' rings (δ 6.23, 7.19) were distinguished from those of C/C' rings (δ 6.75, 6.55) by correlations due to the three-bond couplings with C-2 carbons (δ 114.5, 116.3, 117.2, 120.9) in A/A' and B/B' rings. The H-6' hydrogens from A/A' and B/B' rings were differentiated by the two-bond correlations of the latter with phenyl-ether carbons (δ 147.2, 147.0). The attachment of the two galloyl groups and the valoneoyl A–C and A'–C' rings at the carbon positions of the glucopyranosyl cores were defined by the long-range correlations between carbonyl carbons and the respective aromatic and glucose hydrogens (Table S1).

Conformational analysis

The NMR experiments showed a progressive sharpness of aromatic signals during temperature decrease (from 20 ºC to −20 ºC), which could be explained by the convergence of various oenothein B conformers to a more stable one. To investigate the three-dimensional structure of this conformer, a NOESY experiment was performed at −20 ºC (Figure S4). As expected, the aromatic hydrogens from B, G and A' rings showed strong reciprocal correlations with hydrogens of the glucose cores H-6_I, H-3_{II}, and H-6_{II}, respectively (Figure 3). However, correlations between H-2_I and H-6'$_{C'}$, H-3_I and H-2"/6"$_{G'}$, H-4_I and H-6'$_A$, H-2_{II} and H-6'$_C$, and H4_{II} and H-6'$_{B'}$ were not observed; instead, the signal of H-3_I showed NOE interactions with H-6'$_{B'}$ and H-6'$_A$, whereas H-2_{II} presented a spatial correlation with H-2"/6"$_G$. In addition, four correlations between aromatic hydrogens were detected: H-6'$_A$ and H-2"/6"$_{G'}$, H-6'$_B$ and H-2"/6"$_G$, H-6'$_C$ and H-2"/6"$_G$, and H-6'$_{C'}$ and H-2"/6"$_{G'}$ (Figure 3). These results indicated a spatial proximity of the G galloyl ring with B and C rings from the valoneoyl group, and also that the G ring should be folded toward the H-2 and H-3 hydrogens of glucose II. The G' galloyl group proved spatially close to A and C' rings, although not to hydrogens H-2, H-3, and H-4 of glucose I.

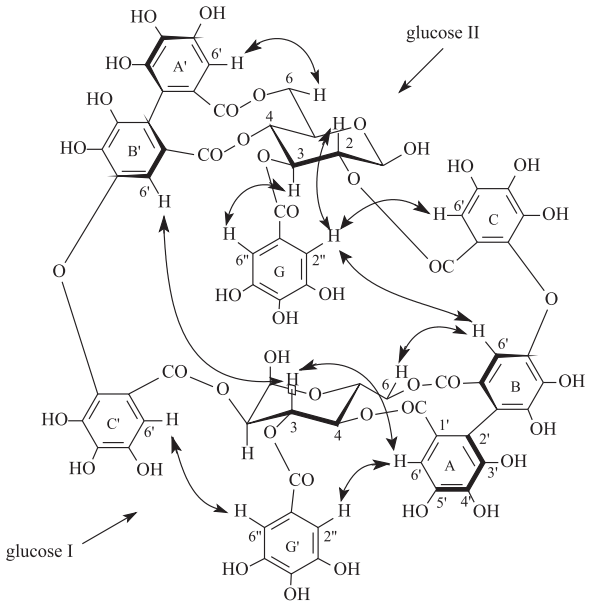

Figure 3. Through-space ^{1}H-^{1}H correlations determined by the NOESY experiment.

Therefore, to describe in further detail the favoured conformation of oenothein B in acetone, geometry optimization was performed using DFT/PCM calculations. The conformer shown in Figure 4 has a compacted structure, resembling a sphere, with the G galloyl ring folded towards the molecular core and the G' galloyl group pointing to the outside. Glucopyranose units adopted standard $^4C_1$ geometries and anomeric hydroxyls did not change their respective configurations during optimization; glucose I and II continued to be α and β, respectively.

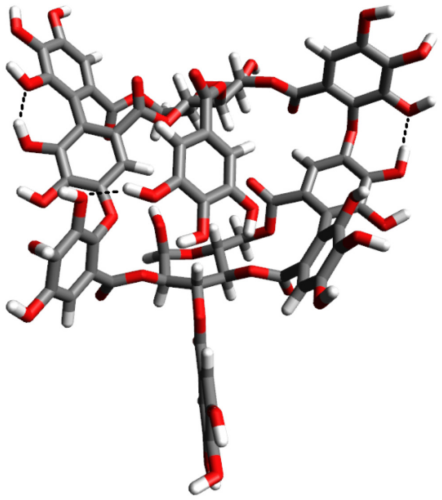

Figure 4. 3D structure of the favoured conformation of oenothein B in acetone.

The position of the G galloyl ring inside the molecule was confirmed by the calculated distances between H-2"$_G$ and H-2_{II}, H-3_{II} and H-6'$_B$, which were 4.45, 2.12, and 3.79 Å, respectively. These distances explained the correlations observed in the NOESY correlation map (Figure 3). The spatial proximity of H-3_I (glucose α) with rings B' and A was also confirmed by the calculated distances of 4.50 Å (H-6'$_{B'}$) and 4.12 Å (H-6'$_A$), which agrees with the NOE correlations observed (Figure 3). Three intramolecular hydrogen bonds were formed between hydroxyl groups at C-3_C and C-4_B (1.71 Å), C-$3_{C'}$ and C-5_G (1.84 Å), and C-$3_{A'}$ and C-$3_{B'}$ (1.71 Å). These intramolecular interactions probably increase the stability of this conformer and contribute to the condensed geometry.

In 2000, Immel and Khanbabaee examined the relative stability of ellagitannin model compounds.[21] Their conformational analysis revealed the rigidity of the hexahydroxydiphenoyl (HHDP) moiety. To compare the stability of the HHDP units of valoneoyl groups in oenothein B with the methyl 4,6-*O*-(*S*)-diphenoyl-β-D-glucoside model, some torsion angles were calculated as in Figure 5.

The HHDP unit of glucose I (α anomer) showed greater deviation in torsion angles Θ_1 and Θ_2 compared with the ellagitannin model (Table 2). The preferred U-shape of both ester groups were achieved in HHDP units of glucoses I and II, with values of Θ_3 and Θ_4 approximated to the ideal 0°. The inclination of carbonyl groups towards the phenoyl rings (Θ_5 and Θ_6) was similar to the model compound,

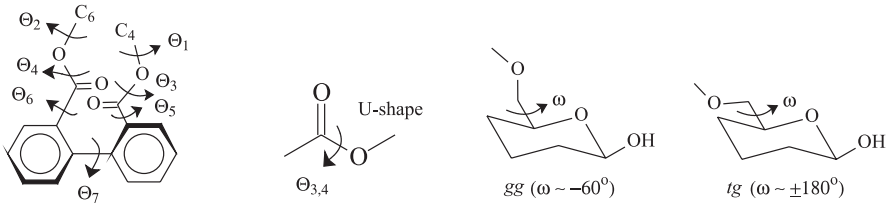

Figure 5. Ring torsion angles Θ_1-Θ_7 and ω used in the geometry analysis. The linkage mode of the diphenoyl-unit to the glucose ring is described by Θ_1 and Θ_2. The most stable U-shape of ester groups is characterized by Θ_3 and Θ_4 with ideal values close to 0º; Θ_5 and Θ_6 indicate the inclination of carbonyl groups towards phenyl rings (ideal values 0º and ± 180º for conjugated π-systems). Positive values for Θ_7 denote the atropisomer *S*. ω values of –60º and ± 180º correspond to *gauche-gauche* (*gg*) and *trans-gauche* (*tg*) forms, respectively.

except for the carbonyl at C-7_A, which inclined almost perpendicularly (Θ_5 = 83.1°) in relation to the A ring plane, preventing the conjugated π-system. The tilt between the phenoyl rings measured about 40-70º (torsion angle Θ_7); positive values indicate (*S*)-HHDP units. The antiparallel arrangement of C=O dipoles (φ = 166º) and the favoured alignment of the ester groups (tilt angleτ_1 = 174º) occurred only in the HHDP unit of glucose II (β anomer). The 6-C-O-linkage in glucose I (α anomer) adopted the less stable *trans-gauche* (*tg*) conformation (ω = 177.9º), whereas the HHDP unit from glucose II is in the preferred *gauche-gauche* (*gg*) form (Figure 5). The comparison showed similar geometry and stability in the HHDP group of glucose II (β anomer) and the ellagitanin model (Table 2).

Table 2. Theoretical geometry parameters for the favoured conformation of oenothein B in acetone

			Glucose I (Valoneoyl ABC)	Glucose II (Valoneoyl A'B'C')	Methyl-4,6(*S*)-DP-β-glucose[a]
Torsion angles / degrees	Θ_1	(C_5-C_4-O-C)	–151.0	–119.0	–130.9
	Θ_2	(C_5-C_6-O-C)	–82.1	–124.9	–111.8
	Θ_3	(C_4-O-C=O)	–8.4	–17.4	–28.9
	Θ_4	(C_6-O-C=O)	1.1	–8.0	–30.5
	Θ_5	(O=C-$C_{1'}$-$C_{2'}$) [b]	83.1	38.2	49.2
	Θ_6	(O=C-$C_{1'}$-$C_{2'}$) [c]	148.9	48.9	36.9
	Θ_7	($C_{1'A}$-$C_{2'A}$-$C_{2'B}$-$C_{1'B}$)	67.5	44.5	56.2
	Θ_8	(C_2-O-C=O)	–11.5	6.3	–
	Θ_9	(C_3-O-C=O) [d]	–1.4	–144.4	–
	Θ_{10}	(O=C-$C_{1'}$-$C_{2'}$) [e]	–25.3	51.0	–
	Θ_{11}	(O=C-$C_{1'}$-$C_{2'}$) [d]	–0.1	26.9	–
	ω	(O_5-C_5-C_6-O_6)	177.9	–89.5	–80.9
	ϕ_1	($C_{2'C}$-O-$C_{5'B}$-$C_{6'B}$)	89.1	–25.2	–
	ϕ_2	($C_{5'B}$-O- $C_{2'C}$- $C_{1'C}$)	–81.9	–55.0	–
Angle / degrees	φ	(C=O / C=O) [f]	118.3	166.3	150.6
	σ	(C-O-C) [g]	118.1	123.4	–
Tilt angle /degrees	τ_1	(C-COO / C-COO) [h]	138.0	174.0	168.5
	τ_2	(phenoyl-O-phenoyl) [i]	121.5	70.8	–

[a]Methyl 4,6-*O*-(*S*)-diphenoyl-β-D-glucoside model;[21] [b]rings A and B'; [c]rings B and A'; [d]rings G' and G; [e]rings C and C'; [f]angle between the bond vectors of ester carbonyl groups; [g]ether linkages between rings C and B, C'and B'; [h]tilt angle between the two planes defined by ester groups (atoms C-COO); [i]tilt angle between the two planes defined by phenoyl groups (rings B and C, B' and C').

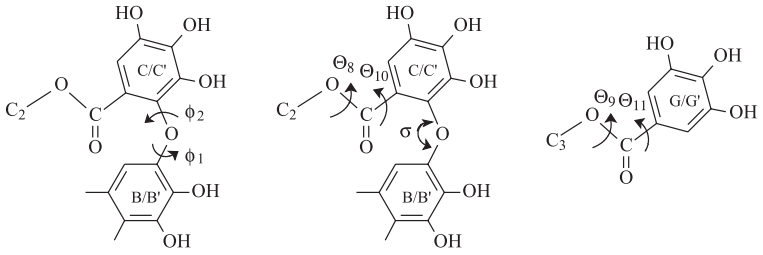

Figure 6. Ring torsion angles Θ_8-Θ_{11} and ϕ_1-ϕ_2, and C–O–C angle σ used in the geometry analysis.

Differences in HHDP geometries and stabilities are due to the changed attachments of the diphenoyl ether bridges. In glucose I, the ether linkage is established between ring B (ester bonded to C-6) and ring C, whereas in glucose II the ether bridge is between ring B' (ester bonded to C-4) and ring C' (Figure 4). As a result of the inversion in the attachment, there is less space for the 6–CH_2–O–CO– fragment of glucose I to adopt the *gg*-form and the antiparallel C=O dipole-dipole alignment, in comparison with the same fragment of glucose II (distances from C-5_I to C-1'$_B$ = 4.51 Å vs. C-5_{II} to C-1'$_{B'}$ = 4.65 Å). As a consequence, the HHDP unit of glucose I is highly compacted and strained.

The ester groups attached to C, C' and G' rings adopted the preferred U-shape, as shown by the small values for torsion angles $\Theta_{8/9}$ (Figure 6 and Table 2). It is worthy of note that the ester fragment linked to the G ring failed to maintain the characteristic U-shape (Θ_9 = −144.4), the reason being the C-7-O linkage turned almost 180º and the galloyl group became oriented towards the middle of the macrocyclic ring. The carbonyl of the G galloyl group was completely conjugated with the phenoyl π-system, whereas carbonyl linked to C' ring showed a 51º deviation from the ideal angle.[21]

The conformation of the ether bridges of the valoneoyl groups was analysed by torsional angles (ϕ_1 and ϕ_2), angles σ (Figure 6), and tilt angles τ_2 between the two planes of rings C/B and C'/B'. In comparison with diphenyl ethers, there are four possible types of conformation: planar ($\phi_1 = \phi_2 = 0º$), butterfly or gable ($\phi_1 = \phi_2 = 90º$), skew ($\phi_1 = 0º$, $\phi_2 = 90º$), and twist ($\phi_1, \phi_2 > 0º$).[22,23] The conformation energy varies from the less stable coplanar form to the minimum "twisted" energy conformation.[22] Polychlorinated biphenyls adopted the skew or twist conformation according to the number of *ortho*-substituents.[24] In the oenothein B structure, the ether bridge between rings C and B assumed the less stable butterfly conformation (ϕ_1, ϕ_2 ca. 90º), whereas the ether linkage C-$6_{B'}$-O-C6'$_{C'}$ was in the preferred twist form (ϕ_1 = −25.2º, ϕ_2 = −55.0º); the latter was in reasonable agreement with experimental and theoretical studies on diphenyl ethers.[25] It is worth mentioning that the two intramolecular hydrogen bonds formed between hydroxyl groups of rings B/C and C'/G restricted the conformations of the ether bridge in the valoneoyl groups (Figure 4).

Conclusions

The use of low temperatures in the NMR experiments of the macrocyclic ellagitannin oenothein B showed significant improvement, mainly in the resolution of the hydrogen spectrum. This technique allowed the confirmation/revision of ^{1}H NMR signals of the entire structure without derivatization or degradative methodologies. The most stable conformer was analysed at −20 ºC and showed a compacted geometry. It was possible to conclude that the mutually reversed orientation of the two valoneoyl groups at the O-4/O-6 position of each glucose core generated differences in the conformational stabilities between the two ether bridges and HHDP groups. Based on the DFT/PCM optimized geometry, it was clear that valoneoyl group ABC (glucose I) had a higher strain than the other A'B'C' group (glucose II). This conformational analysis will be useful in further investigations on interactions between oenothein B and different receptors, as this compound is considered a promising lead for further therapeutic development.[8]

Supplementary Information

Supplementary information (Figures S1-S4 and Table S1) is available free of charge at http://jbcs.org.br as a PDF file.

Acknowledgements

The authors wish to thank Prof Dr Luiz Henrique Keng Queiroz Jr. for assistance with NMR informations and Conselho de Aperfeiçoamento do Ensino Superior (CAPES) for granting a fellowship to A.G.C. and G.A.C.F.

References

1. Hatano, T.; Yasuhara, T.; Matsuda, M.; Yazaki, K.; Yoshida, T.; Okuda, T.; *J. Chem. Soc. Perkin Trans I* **1990**, 2735.

2. Yoshida, T.; Chou, T.; Nitta, A.; Okuda, T.; *Chem. Pharm. Bull.* **1992**, *40*, 2023.
3. Yoshida, T.; Maryuama, T.; Nitta, A.; Okuda, T.; *Chem. Pharm. Bull.* **1992**, *40*, 1750.
4. Santos, S. C.; Waterman, P. G.; *Fitoterapia* **2001**, *72*, 95.
5. Lee, M. H.; Nishimoto, S.; Yang, L. L.; Yen, K. Y.; Hatano, T.; Yoshida,T.; Okuda, T.; *Phytochemistry* **1997**, *44*, 1343; Chen, L. G.; Yen, K. Y.; Yang, L. L.; Hatano, T.; Okuda, T.; Yoshida, T.; *Phytochemistry* **1999**, *50*, 307; Lesuisse, D.; Berjonneau, J.; Ciot, C.; Devaux, P.; Doucet, B.; Gourvest, F.; Khemis, B.; Lang, C.; Legrand, R.; Lowinski, M.; Maquin, P.; Parent, A.; Schoot, B.; Teutsch, G.; *J. Nat. Prod.* **1996**, *59*, 490; Ducrey, B.; Marston, A.; Göhring, S.; Hartmann, R.W.; Hostettmann, K.; *Planta Med.* **1997**, *63*, 111.
6. Wang, C. C.; Chen, L. G.; Yang, L. L.; *Cancer Lett.* **1999**, *140*, 195; Yang, L. L.; Wang, C. C.; Yen, K. Y.; Yoshida, T.; Hatano, T.; Okuda, T.; *Basic Life Sci.* **1999**, *66*, 615; Sakagami, H.; Jiang, Y.; Kusama, K.; Atsumi, T.; Ueha, T.; Toguchi, M.; Iwakura, I.; Satoh, K.; Ito, H.; Hatano, T.; Yoshida, T.; *Phytomedicine* **2000**, *7*, 39.
7. Miyamoto, K.; Murayama, T.; Nomura, M.; Hatano, T.; Yoshida, T.; Furukawa, T.; Koshiura, R.; Okuda, T.; *Anticancer Res.* **1993**, *13*, 37; Miyamoto, K.; Nomura, M.; Sasakura, M.; Matsui, E.; Koshiura, R.; Murayama, T.; Furukawa, T.; Hatano, T.; Yoshida, T.; Okuda, T.; *Jpn. J. Cancer Res.* **1993**, *84*, 99.
8. Schepetkin, I.A.; Kirpotina, L. N.; Jakiw, L.; Khlebnikov, A. I.; Blaskovich, C. L.; Jutila, M. A.; Quinn, M.T.; *J. Immunol.* **2009**, *183*, 6037.
9. Aoki, K.; Maruta, H.; Uchiumi, F.; Hatano, T.; Yoshida, T.; Tanuma, S.; *Biochem. Biophys. Res. Comm.* **1995**, *210*, 329; Lee, M. H.; Chiou, J. F.; Yen, K. Y.; Yang, L. L.; *Cancer Lett.* **2000**, *154*, 131.
10. Kiss, A. K.; Bazylko, A.; Filipek, A.; Granica, S.; Jaszewska, E.; Kiarszys, U.; Kósmider, A.; Piwowarski, J.; *Phytomedicine* **2011**, *18*, 557.
11. Fukuchi, K.; Sakagami, H.; Okuda, T.; Hatano, T.; Tanuma, S.; Kitajima, K.; Inoue, Y.; Inoue, S.; Ichikawa, S.; Nonoyama, M.; Konno, K.; *Antiviral Res.* **1989**, *11*, 285; Santos, G. D., Santos, S. C.; Ferri, P. H.; Soares, C. M. A.; Pereira, M.; *Med. Mycol.* **2007**, *45*, 609.
12. Yoshida, T.; Chou, T.; Nitta, A.; Miyamoto, K.; Koshiura, R.; Okuda, T.; *Chem. Pharm. Bull.* **1990**, *38*, 1211.
13. Yoshida, T.; Hatano, T.; Okuda, T.; *Magn. Reson. Chem*. **1992**, *30*, S46.
14. http://www.acdlabs.com accessed in June 2013.
15. Frisch, M. J.; Trucks, G. W.; Schlegel, H. B.; Scuseria, G. E.; Robb, M. A.; Cheeseman, J. R.; Scalmani, G.; Barone, V.; Mennucci, B.; Petersson, G. A.; Nakatsuji, H.; Caricato, M.; Li, X.; Hratchian, H. P.; Izmaylov, A. F.; Bloino, J.; Zheng, G.; Sonnenberg, J. L.; Hada, M.; Ehara, M.; Toyota, K.; Fukuda, R.; Hasegawa, J.; Ishida, M.; Nakajima, T.; Honda,Y.; Kitao, O.; Nakai, H.; Vreven,T.; Montgomery, Jr., J. A.; Peralta, J. E.; Ogliaro, F.; Bearpark, M.; Heyd, J. J.; Brothers, E.; Kudin, K. N.; Staroverov, V. N.; Kobayashi, R.; Normand, J.; Raghavachari, K.; Rendell, A.; Burant, J. C.; Iyengar, S. S.; Tomasi, J.; Cossi, M.; Rega, N.; Millam, J. M.; Klene, M.; Knox, J. E.; Cross, J. B.; Bakken, V.; Adamo, C.; Jaramillo, J.; Gomperts, R.; Stratmann, R. E.; Yazyev, O.; Austin, A. J.; Cammi, R.; Pomelli, C.; Ochterski, J. W.; Martin, R. L.; Morokuma, K.; Zakrzewski, V. G.; Voth, G. A.; Salvador, P.; Dannenberg, J. J.; Dapprich, S.; Daniels, A. D.; Farkas, O.; Foresman, J. B.; Ortiz, J. V.; Cioslowski, J.; Fox, D. J.; Gaussian, Inc., Wallingford CT, 2009.
16. Tomasi, J.; Mennucci, B.; Cammi, R.; *Chem. Rev.* **2005**, *105*, 2999.
17. avogadro.openmolecules.net accessed in November 2013.
18. Waterman, P. G.; Crichton, E. G.; *Phytochemistry* **1980**, *19*, 2723; Li, X. C.; Joshi, A. S.; Tan, B.; ElSohly, H. N.; Walker, L. A.; Zjawiony, J. K.; Ferreira, D.; *Tetrahedron* **2002**, *58*, 8709.
19. Kleinpeter, E.; Heydenreich, M.; Koch, A.; Linker, T.; *Tetrahedron* **2012**, *68*, 2363.
20. Wagner, G.; Feigel, M.; *Tetrahedron* **1993**, *49*,10831; Konishi, H.; Hashimoto, S.; Sakakibara, T.; Matsubara, S.; Yasukawa, Y.; Morikawa, O.; Kobayashi, K.; *Tetrahedron Lett.* **2009**, *50*, 620; Faraldos, J. A.; Wu, S.; Chappell, J.; Coates, R. M.; *Tetrahedron* **2007**, *63*, 7733.
21. Immel, S.; Khanbabaee, K.; *Tetrahedron: Asymmetry* **2000**, *11*, 2495.
22. Paiva, A.C.S.; Kistemaker, P.G.; Weeding, T.L.; *Int. J. Mass Spectrom*. **2002**, *221*,107.
23. Hu, J.; Eriksson, L.; Bergman, A.; Kolehmainen, E.; Knuutinen, J.; Suontamo, R.; Wei, X.; *Chemosphere* **2005**, *59*, 1033.
24. Nevalainen, T.; Rissanen, K.; *J. Chem. Soc., Perkin Trans.* **1994**, *2*, 271.
25. Schaefer, T.; Penner, G.H.; Takeuchi, C.; Tseki, P.; *Can. J. Chem.* **1988**, *66*, 1647.

Submitted: August 5, 2013
Published online: December 13, 2013